

F-3-3

Behavior of Plated Micro-Bumps during Ultrasonic Flip-Chip Bonding Determined from Dynamic Strain Measurement

Naoya Watanabe and Tanemasa Asano

Center for Microelectronic Systems, Kyushu Institute of Technology
680-4 Kawazu, Iizuka, Fukuoka 820-8502, Japan

Phone: +81-948-29-7589, Fax: +81-948-29-7586, E-mail: naoya@cms.kyutech.ac.jp

1. Introduction

In order to realize three-dimensionally stacked-chip system in a package, the bonding technology with a high I/O number is required. The ultrasonic flip-chip bonding has great potential to facilitate three-dimensional chip stacking¹⁾ because it possesses the following advantage; 1) simple process, 2) low processing temperature, 3) low attenuation of high frequency signals.

However the bonding mechanism of the ultrasonic flip-chip bonding has not been clarified yet. We have been investigating bonding behavior by measuring dynamic strain and its distribution generated under a bump during ultrasonic flip-chip bonding.^{2,3)} This method has been found to be very useful for investigating the bonding behavior of bumps. We have clarified the bonding behavior of large-bump made of Au.

In this paper, the bonding of micro-bump prepared by electroplating is investigated. Dynamic strain generated under a plated micro-bump is measured using Si thin-film gauge array. Comparative study between large-bump and micro-bump clearly demonstrates the difference in bonding behavior. The results of this study will contribute to realizing stacked-chips with high-number of inter-layer connections.

2. Experimental

Figure 1(a) shows an optical micrograph of the strain gauge array covered with Al bonding pad, which was fabricated on SOI to measure the dynamic strain and its distribution generated under a plated micro-bump during ultrasonic flip-chip bonding. One segment of this array is composed of a pair of p-type and n-type gauges to detect two-directional strain as is described below. The pairs of gauge are 10 μm long and form chain to measure the strain distribution under a bump.

Figure 1(b) shows the schematic illustration of this array. The longitudinal axes of p-type and n-type gauges are aligned in the [110] direction on the Si (001) substrate. With this configuration, each gauge possesses the piezoresistance coefficients shown in Fig. 1(c).⁴⁾ Thus, when we apply ultrasonic vibration along x-axis (longitudinal axis), ε_x and ε_z are determined from the resistance changes of these two gauges because ε_y is much smaller than ε_x and ε_z .

On the Si substrate with this strain gauge array, one of plated micro-bumps arrayed on a chip was bonded as shown in Fig. 2. The bump material was Au.

3. Dynamic strain under a plated micro-bump

Figure 3 shows the distribution of dynamic strain generated under a plated micro-bump. (a) and (b) correspond to the strain generated at the positions 0 μm and 10 μm from the center of the bump ($\approx 33 \mu\text{m}$ square), respectively. The measured time-evolution of strain can be divided into 3 steps; (1)pre-press step, (2)ultrasonic

step and (3)post-press step of the bonding sequence. In ultrasonic step, the strain oscillates in accordance with the ultrasonic vibration.

The strain vibrations generated at each position are almost the same. This indicates that, in the case of plated bump, the ultrasonic vibration and pressing load are uniformly applied to the bump. The time evolution of strain vibration shows that the magnitude of strain vibration suddenly drops at 50 ms from the beginning of ultrasonic application. This change is considered to be due to the bonding of bump. The large strain generated from 0 ms to 50 ms is considered to be due to the deformation of the bump. This behavior of the plated micro-bump is different from that of ball bump as shown below.

4. Comparison with strain under a large-bump

It has been found that, even when the size of the plated bump is large ($\approx 100 \mu\text{m}$ square), the bonding behavior is the same as that shown in Fig. 3.

On the other hand, there appeared a quite difference in dynamic strain between ball bump and plated micro-bump. Figure 4 shows the distribution of dynamic strain generated under a ball bump. Bonding of ball bump was carried out under larger pressure than that of plated micro-bump. (a)-(c) correspond to the strain generated at the positions 0 μm , 20 μm and 40 μm from the center of the bump ($\approx 100 \mu\text{m}$ in a diameter), respectively. Comparing Fig. 3 with Fig. 4, we find the following two differences in dynamic strain. First is the distribution of strain vibration. In the case of ball bump, the strain vibration at the periphery of bump is different from that at the center of bump. This is quite different from the behavior of the plated micro-bump, where the distribution of the strain vibration is uniform. Second is the time evolution of strain vibration. The large strain vibration is generated over the period of ultrasonic application in the case of ball bump, while the strain vibration drops after about 50 ms in the case of plated micro-bump. From these observations, we can figure out the bonding behavior of ball bump and plated micro-bump as illustrated in Fig. 5.

In the case of ball bump which has round surface, a large deformation of the bump surface occurs at the periphery of bump because ball bump expands outside by plastic flow. On the other hand, in the case of plated micro-bump which has flat surface, plastic flow hardly occurs and a small deformation of the bump surface occurs uniformly by friction. This difference in bonding behavior can explain the fact that the bonding of plated micro-bump required a smaller pressure during ultrasonic application than ball bump.

Figures 6(a) and 6(b) show the SEM images of ball bump and plated micro-bump, respectively. These SEM images assure the difference in bonding behavior between ball bump and plated micro-bump.

5. Conclusion

Dynamic strain generated under a Au plated micro-bump during ultrasonic flip-chip bonding has been measured using Si thin-film strain gauge to investigate its bonding behavior. Results have revealed that plated micro-bump bonds with small deformation of bump surface produced by friction. The bonding behavior of plated micro-bump has been found to be the same as that of plated large bump and quite different from that of ball bump. This difference in bonding behavior can clearly explain why the bonding of plated micro-bump required a smaller pressure during ultrasonic application than ball bump.

References

- [1] K. Tanida et al.: *2002 International Conference on Electronics Packaging*, (2002) p. 333-338.
- [2] M. Hizukuri, N. Watanabe and T. Asano: *Jpn. J. Appl. Phys.* **40** (2001) 3044.
- [3] N. Watanabe and T. Asano: *2002 International Conference on Electronics Packaging*, (2002) p. 381-385.
- [4] C. S. Smith : *Phys. Rev.* Vol. **94** (1954) p. 42.

Acknowledgment

This work was supported in part by the Grant-in-Aid for Scientific Research (No. 14040216) from the Ministry of Education, Culture, Sports, Science and Technology.

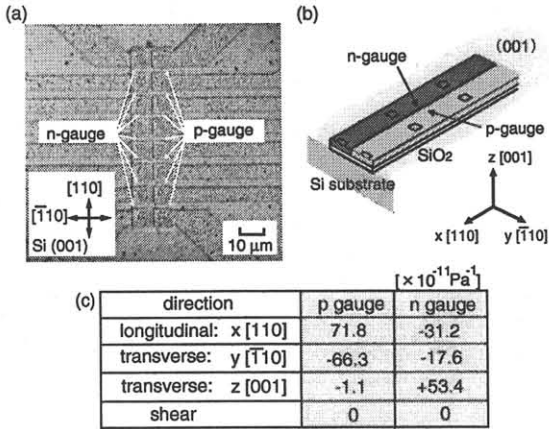


Fig. 1: (a) An optical micrograph of strain gauge covered with Al bonding pad. (b) Schematic illustration of the strain gauge array. (c) Piezoresistance coefficients of Si gauges aligned in the [110] direction on (001) Si substrate.

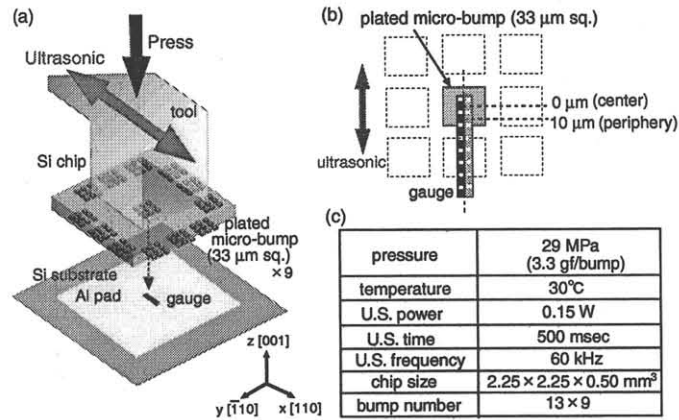


Fig. 2: (a) The chip/substrate configuration. (b) The relative position between the bump and the strain gauge. (c) Bonding condition.

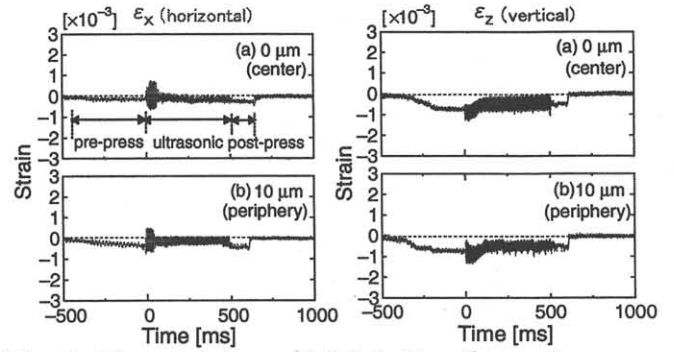


Fig. 3: Time evolution and distribution of ϵ_x and ϵ_z generated under a plated micro-bump.

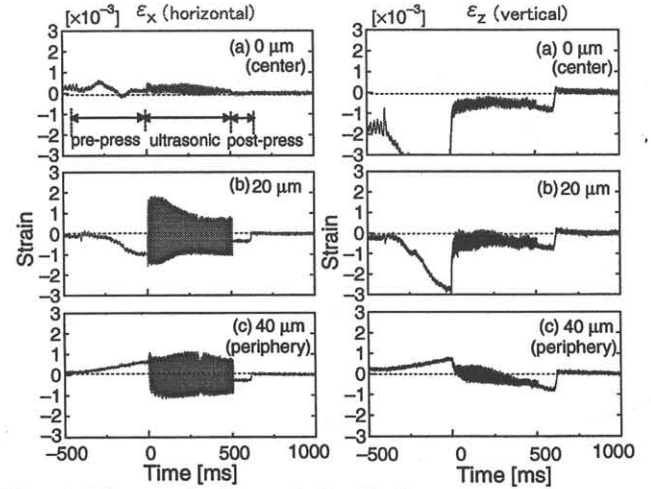


Fig. 4: Time evolution and distribution of ϵ_x and ϵ_z generated under a ball bump.

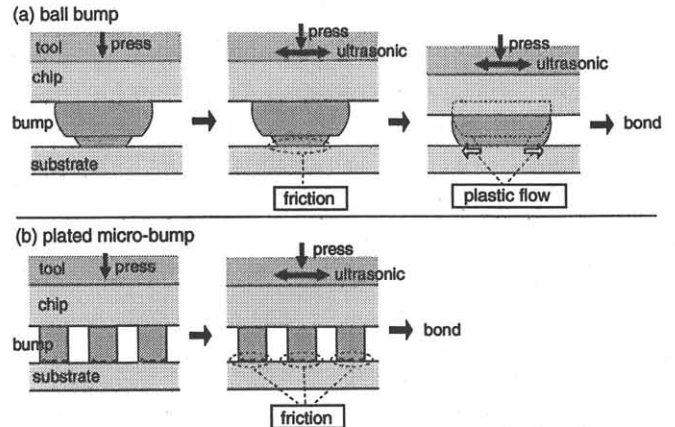
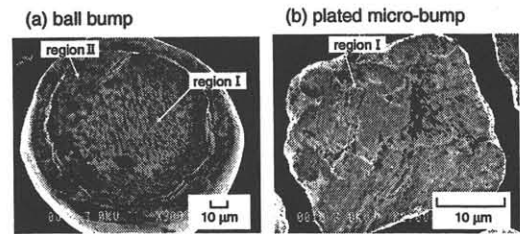


Fig. 5: Bonding behavior of ball bump and plated micro-bump. (a): ball bump. (b): plated micro-bump.



* region I: region formed by friction
* region II: region formed by plastic flow

Fig. 6: SEM image of bonded area (bump surface). (a): ball bump. (b): plated micro-bump.